# Journal of Materials Chemistry C

## COMMUNICATION

Check for updates

# Complete self-recovery of photoluminescence of photodegraded cesium lead bromide quantum dots†

Koji Kidokoro, Yoshiki Iso [iD] * and Tetsuhiko Isobe [iD] *

CsPbBr₃ quantum dots were packed in a cell and irradiated at 468 nm. The sample color changed to black, attributed to the formation of surface defects by photoinduced desorption of surface ligands. The color and photoluminescence properties completely recovered during subsequent dark storage. This can be explained by readsorption of the surface ligands.

All-inorganic perovskite $CsPbX_3$ (X = Cl, Br, I) nanocrystals have attracted great interest as fluorescent quantum dots (QDs) since Kovalenko and colleagues published their sensational report in 2015.[1] Colloidal fluorescent $CsPbX_3$ QDs have frequently been prepared *via* the hot injection method proposed by Kovalenko's group and modified by other researchers. The QDs have a direct transition type and exhibit highly efficient photoluminescence (PL) with a very narrow peak width. The most characteristic property of the QDs is facile control of their light absorption and PL wavelengths by adjusting their band gap through halide anion exchange.[2] These excellent properties have attracted much attention, especially in applications for LEDs,[3,4] wide-color gamut displays,[1] photovoltaic devices,[5] lasers,[6,7] photodetectors,[8] photocatalysts,[9] and bioimaging;[10] therefore, $CsPbX_3$ QDs have been examined by many research groups.[11–17] Furthermore, other cesium lead halides, *e.g.*, $CsPb_2Br_5$,[18] are also attractive in optoelectronic devices. In $CsPbX_3$, green-emitting bromide QDs show a higher PL quantum yield (PLQY) and stability than the chloride and iodide QDs. Furthermore, the pure-green emission from $CsPbBr_3$ QDs has a narrower peak width ($\sim$20 nm) than that of ternary copper chalcogenide QDs and InP QDs, which have been developed as Cd-free visible-light-emitting phosphors.[19–23]

All-inorganic $CsPbBr_3$ QDs have better stability than conventional organic–inorganic lead bromide perovskite QDs developed

*Department of Applied Chemistry, Faculty of Science and Technology,*
*Keio University, 3-14-1 Hiyoshi, Kohoku-ku, Yokohama 223-8522, Japan.*
*E-mail: iso@applc.keio.ac.jp, isobe@applc.keio.ac.jp*
† Electronic supplementary information (ESI) available: Experimental details, supporting texts, Fig. S1–S7, and Tables S1 and S2. See DOI: 10.1039/c9tc02365h

for solar devices; nevertheless, the ready degradation of these QDs under light irradiation is a significant problem preventing their practical use. The photostability of $CsPbBr_3$ QDs has been improved by formation of a QD core/shell structure,[24] passivating the QDs with a metal complex,[25] and embedding the QDs into a matrix such as silica, aluminosilicate, or polymer resin,[26–28] but complete suppression of photodegradation is still challenging. Furthermore, photodegradation is generally an irreversible phenomenon suffered by various nanophosphors; therefore, the recovery of degraded QDs is of significance. In this report, we discovered complete self-recovery of the PL properties of $CsPbBr_3$ QDs degraded by excitation light. Stability is one of the most important problems of nanometer-sized fluorescent materials because they are significantly affected by their surroundings due to their large specific surface area, and to the best of our knowledge, such a drastic self-recovery phenomenon has not been previously observed. To investigate the interesting phenomena of $CsPbBr_3$ QD photodegradation and subsequent self-recovery, we evaluated the changes in the crystal structure, morphology, ligand adsorption, UV-vis light absorption, and PL properties.

$CsPbBr_3$ perovskite QDs capped with oleate anions and oleylammonium cations, which are deprotonated oleic acid and protonated oleylamine, respectively, were prepared by the hot injection method. The resulting QD sample, which was yellow in color and showed green PL emission, was placed in a powder cell and irradiated by a 468 nm blue, flat LED panel for 72 h (Fig. S1, ESI†). Details of these experimental methods and conditions are described in the ESI.† Fig. 1a shows the change in the body color of the QDs during the blue LED irradiation period and subsequent storage in the dark. The sample color changed from yellow to black during irradiation. According to the thermal images (Fig. S2, ESI†), the thermal damage to the sample was negligible. Therefore, the degradation of the QDs can be attributed only to photodegradation. The photodegraded sample exhibited gradual recovery without any treatment during storage in the dark at room temperature. The as-prepared QDs exhibited UV-vis light absorption at $\sim$550 nm and shorter wavelengths (Fig. 1b), which can be attributed to the inter-band
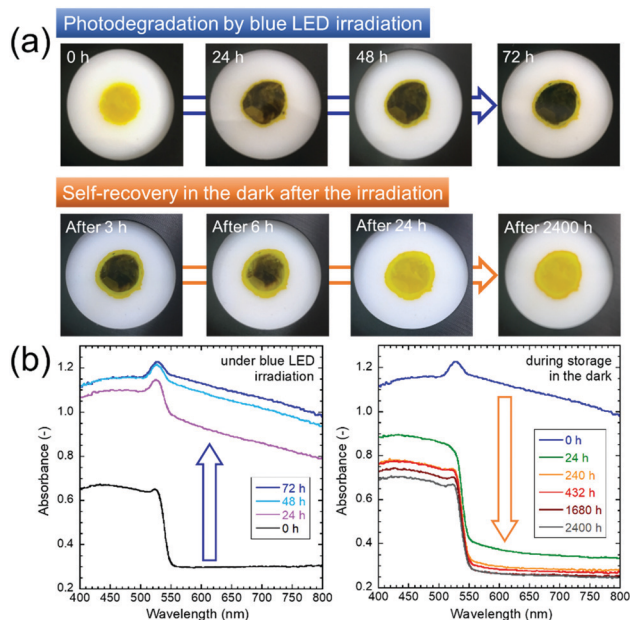
Fig. 1 (a) Photographs of the photodegradation of the QD samples during blue LED irradiation for 72 h and the subsequent self-recovery during storage in the dark for 2400 h. (b) Corresponding change in the UV-vis absorption spectra of the QDs.

transition of the CsPbBr$_3$ QDs, while no absorption was observed in the longer wavelength region, resulting in the yellow color.

The band gap of the as-prepared QD sample was estimated to be 2.27 eV from the Tauc plot, which was created from the UV-vis spectrum (Fig. S3, ESI†). The band gap was larger than the calculated 2.00 eV of bulk cubic CsPbBr$_3$,[1] revealing the quantum size effect. During continuous blue-light irradiation for 72 h, the absorbance increased over the whole region, which was consistent with the black color. A small peak at ~530 nm, which can be assigned to the exciton peak of the QDs, remained after photodegradation. However, the absorbance enhancement in the region above ~550 nm was not associated with the intrinsic properties of the CsPbBr$_3$ QDs. Gradual recovery of UV-vis absorption spectra was observed during storage in the dark.

Drastic changes in the PL intensity were also observed. The PL spectrum of the QDs (Fig. 2a) had a sharp emission peak at ~520 nm. Notably, a shoulder peak, which does not appear in the PL spectrum of the CsPbBr$_3$ QD dispersion,[29] was observed (see ESI†). The PL intensity decreased to ~20% its initial value as the UV-vis absorbance increased upon blue LED irradiation. The remaining PL emission may come from undamaged QDs in deeper positions of the sample in the cell. Gradual recovery of the PL intensity after storage in the dark for 2400 h resulted in an intensity value that was 108% of the initial value. The PL lifetimes were also evaluated from the PL decay curves to investigate the influence of surface defects (Fig. 2b). A significant change was observed after the 72 h irradiation period, and the PL lifetime recovery during subsequent storage in the dark was confirmed. Detailed results for the PL lifetimes and amplitudes
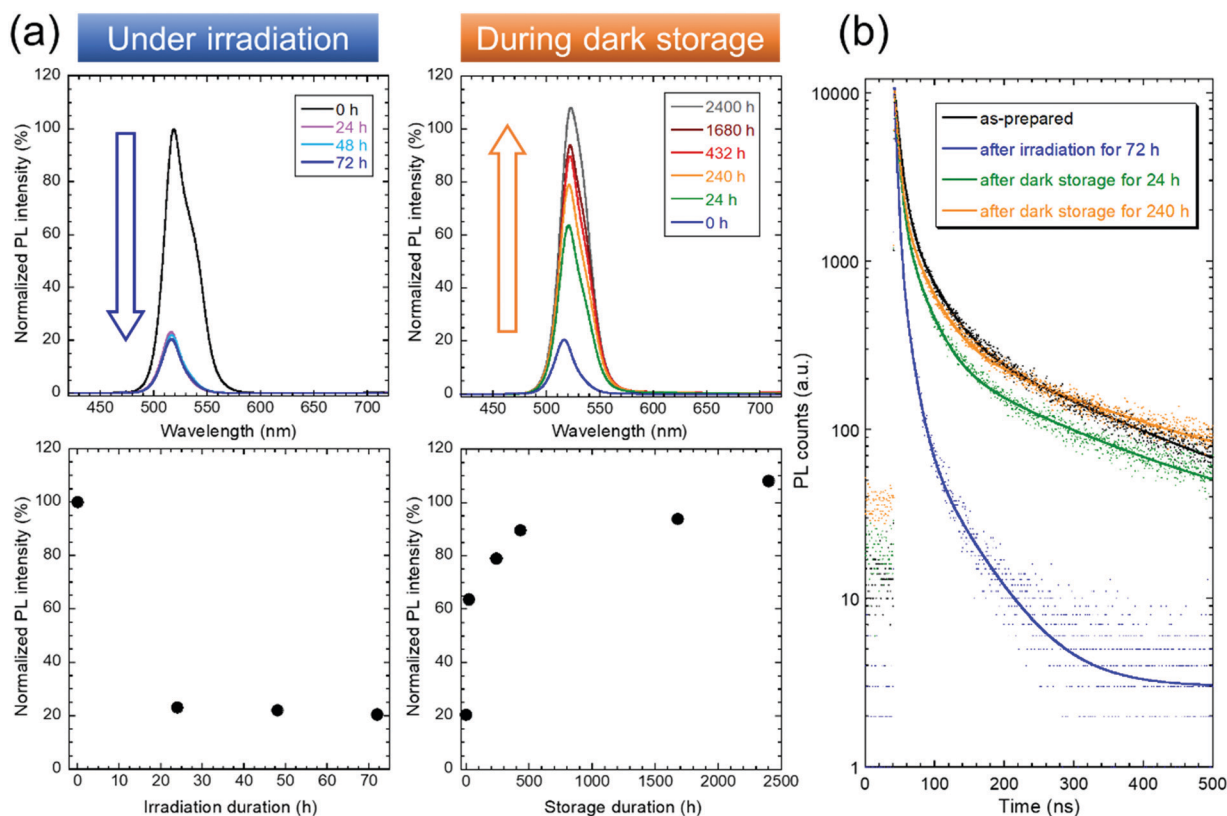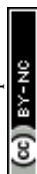


Fig. 2 Changes in the PL properties of the QDs before and after blue LED irradiation for 72 h and during subsequent storage in the dark. (a) PL spectra ($\lambda_{ex}$ = 468 nm) and peak intensities. (b) PL decay curves.

This journal is © The Royal Society of Chemistry 2019

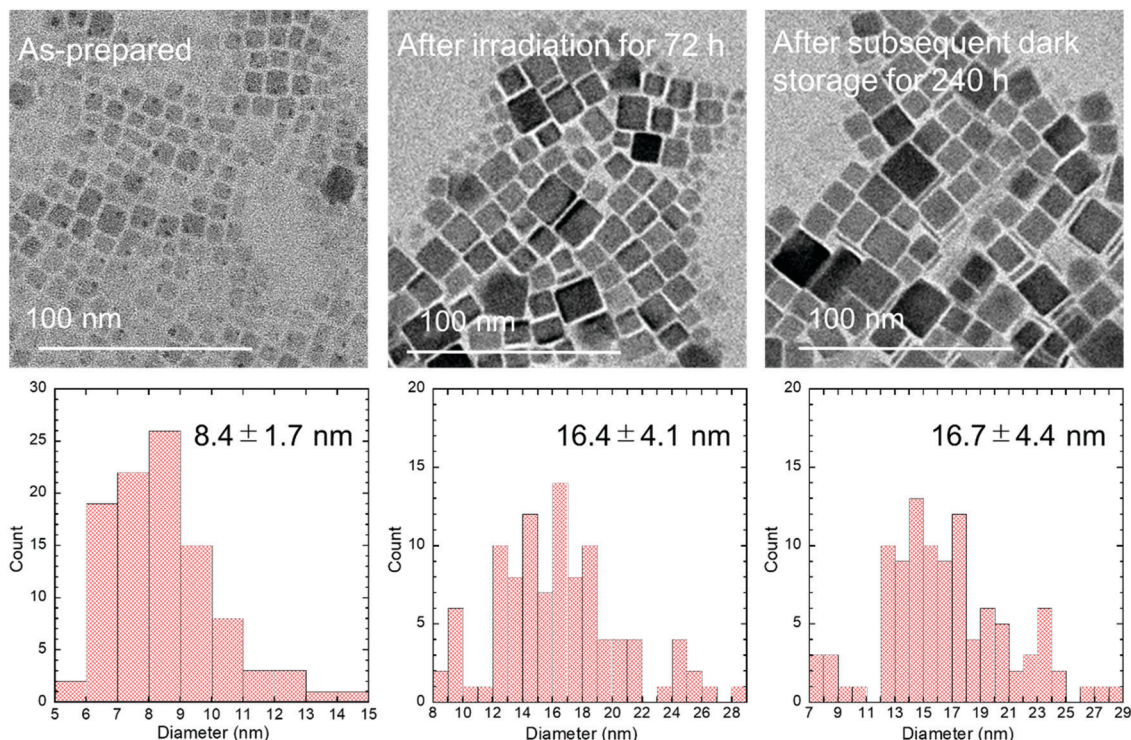J. Mater. Chem. C, 2019, 7, 8546–8550 | 8547

Fig. 3  TEM images and corresponding size distributions of the QDs before and after blue LED irradiation for 72 h and after subsequent storage in the dark for 240 h.

calculated from the curves are summarized in Table S1, ESI.† The initial average PL lifetime (103.9 ns) decreased to 13.2 ns after irradiation for 72 h, followed by an increase to 105.3 ns, which was close to the initial lifetime, after storage in the dark for 240 h. The decrease in the PL lifetime indicates the generation of surface defects that cause PL quenching through nonradiative transitions. These generated surface defects may be color centers, which explains the blackening of the QDs under irradiation. Therefore, the increase in the PL lifetime during storage in the dark reveals that the recovery of sample color from black to yellow may be caused by the disappearance of surface defects. This mechanism should explain the abovementioned changes in the UV-vis absorption and PL properties.

The as-prepared nanocrystals had an average size of $8.4 \pm 1.7$ nm that increased to $16.4 \pm 4.1$ nm after irradiation according to transmission electron microscopy (TEM) images (Fig. 3). Furthermore, the particles remained unchanged after storage in the dark. The growth of rectangular $CsPbBr_3$ QDs is possibly due to exposed crystal surfaces combining after the removal of the surface ligands. This phenomenon of removal of the surface ligands is known as photoinduced desorption.[30,31]

Photoinduced desorption of surface ligands during the crystal growth process resulted in the formation of defects on the QD surfaces, leading to the observed photodegradation. Additionally, the desorbed ligands might adsorb on the exposed surface, allowing self-recovery of PL during storage in the dark. The recovery of the PL intensity over 100% after self-recovery might be due to the optimized coordination states of the readsorbed surface ligands. To further understand the photo-degradation and self-recovery processes, the origin of the generated defects was investigated. Fig. 4a shows the changes in the Fourier transform infrared (FT-IR) spectra of the QDs. A new peak assigned to $\nu(C{=}O)$ appeared at $\sim 1710$ cm$^{-1}$ after LED irradiation, indicating a change in the coordination state of the adsorbed oleate ligand, as illustrated in Fig. 4b. The oleate ligand desorbed by irradiation can be stabilized as oleic acid by receiving protons from nearby oleylammonium ligands. Simultaneously, the desorbed oleylammonium ligand is deprotonated by the oleate ion to form oleylamine. A gradual decrease in the peak of $\nu(C{=}O)$ was observed during storage in the dark, and the decrease is possibly due to partial read-sorption of the oleate ligand, which reverted from oleic acid. Oleylammonium might be readsorbed on the QDs at the same time. Unfortunately, we could not detect any NH vibrational peaks derived from the oleylammonium ligand by FT-IR analysis, which is possibly due to the small amount of the ligand on the QDs. The peak of $\nu(C{=}O)$ did not completely disappear because some of the desorbed ligands could not readsorb on the larger QDs, which had smaller specific surface areas than the as-prepared QDs before irradiation. We hypothesized that photodegradation was caused by the photoinduced desorption of organic ligands, which resulted in the generation of surface defects. The recovery might be due to the return of the coordination state accompanied by the disappearance of the dangling bond.

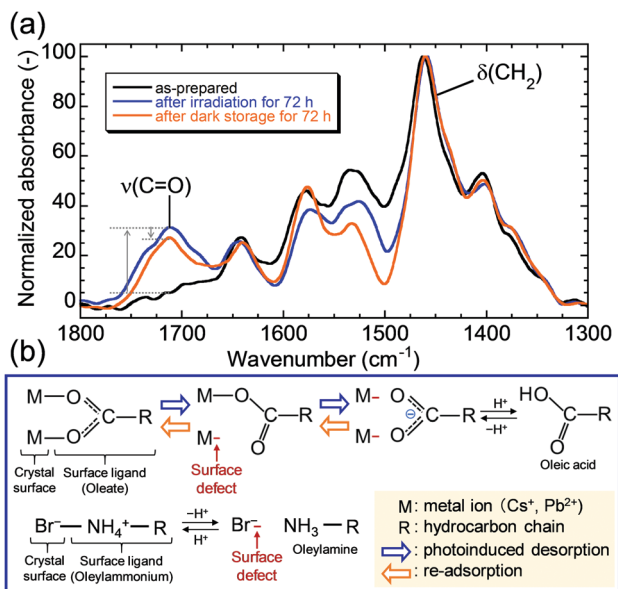It should be noted that the outer edge of the sample remained yellow throughout the entire process, as shown in

8548 | J. Mater. Chem. C, 2019, 7, 8546–8550

This journal is © The Royal Society of Chemistry 2019

Fig. 4 (a) FT-IR spectra of QDs before and after blue LED irradiation for 72 h. $\nu$ = stretching; $\delta$ = deformation. (b) Proposed schematic illustration of the change in the coordination state of the surface ligands on the QDs.

Fig. 1a. The annular yellow part might be degraded through an irreversible oxidation reaction with residual ambient air in the sample cell. When QDs were exposed to ambient air during the blue LED irradiation period, the sample color did not change to black (Fig. S4a, ESI†). Blackening of the sample was not observed, but the PL intensity decreased (Fig. S4b, ESI†). Furthermore, the absorption and PL properties did not recover during subsequent storage in the dark, possibly indicating that the QDs degraded through an irreversible oxidation reaction with damage by moisture under ambient air.[32] The oxidized surface prevented the formation of a color center and could not return to its previous state; therefore, the observed blackening and self-recovery phenomena require an air-free environment. These studies on the drastic self-recovery behavior of CsPbBr$_3$ QDs after significant photodegradation will help further develop their usability.

## Conflicts of interest

There are no conflicts to declare.

## Acknowledgements

## Notes and references

1 L. Protesescu, S. Yakunin, M. I. Bodnarchuk, F. Krieg, R. Caputo, C. H. Hendon, R. X. Yang, A. Walsh and M. V. Kovalenko, *Nano Lett.*, 2015, **15**, 3692–3696.

2 Q. A. Akkerman, V. D'Innocenzo, S. Accornero, A. Scarpellini, A. Petrozza, M. Prato and L. Manna, *J. Am. Chem. Soc.*, 2015, **137**, 10276–10281.

3 D. Yan, T. Shi, Z. Zang, T. Zhou, Z. Liu, Z. Zhang, J. Du, Y. Leng and X. Tan, *Small*, 2019, **15**, 1901173.

4 C. Li, Z. Zang, W. Chen, Z. Hu, X. Tang, W. Hu, K. Sun, X. Liu and W. Chen, *Opt. Express*, 2016, **24**, 15071–15078.

5 A. Swarnkar, A. R. Marshall, E. M. Sanehira, B. D. Chernomordik, D. T. Moore, J. A. Christians, T. Chakrabarti and J. M. Luther, *Science*, 2016, **354**, 92–95.

6 S. Yakunin, L. Protesescu, F. Krieg, M. I. Bodnarchuk, G. Nedelcu, M. Humer, G. de Luca, M. Fiebig, W. Heiss and M. V. Kovalenko, *Nat. Commun.*, 2015, **6**, 8056.

7 C. Li, Z. Zang, C. Han, Z. Hu, X. Tang, J. Du, Y. Leng and K. Sun, *Nano Energy*, 2017, **40**, 195–202.

8 P. Ramasamy, D.-H. Lim, B. Kim, S.-H. Lee, M.-S. Lee and J.-S. Lee, *Chem. Commun.*, 2016, **52**, 2067–2070.

9 Y.-F. Xu, M.-Z. Yang, B.-X. Chen, X.-D. Wang, H.-Y. Chen, D.-B. Kuang and C.-Y. Su, *J. Am. Chem. Soc.*, 2017, **139**, 5660–5663.

10 H. Zhang, X. Wang, Q. Liao, Z. Xu, H. Li, L. Zheng and H. Fu, *Adv. Funct. Mater.*, 2017, **27**, 1604382.

11 M. V. Kovalenko, L. Protesescu and M. I. Bodnarchuk, *Science*, 2017, **358**, 745–750.

12 H. Huang, L. Polavarapu, J. A. Sichert, A. S. Susha, A. S. Urban and A. L. Rogach, *NPG Asia Mater.*, 2016, **8**, e328.

13 S. Ananthakumar, J. R. Kumar and S. M. Babu, *J. Photonics Energy*, 2016, **6**, 042001.

14 X. He, Y. Qiu and S. Yang, *Adv. Mater.*, 2017, **29**, 1700775.

15 X. Li, F. Cao, D. Yu, J. Chen, Z. Sun, Y. Shen, Y. Zhu, L. Wang, Y. Wei, Y. Wu and H. Zeng, *Small*, 2017, **13**, 1603996.

16 Y. Iso and T. Isobe, *ECS J. Solid State Sci. Technol.*, 2017, **7**, R3040–R3045.

17 T. Chiba and J. Kido, *J. Mater. Chem. C*, 2018, **6**, 11868–11877.

18 C. Han, C. Li, Z. Zang, M. Wang, K. Sun, X. Tang and J. Du, *Photonics Res.*, 2017, **5**, 473–480.

19 C. Coughlan., M. Ibáñez, O. Dobrozhan, A. Singh, A. Cabot and K. M. Ryan, *Chem. Rev.*, 2017, **117**, 5865–6109.

20 C. Wada, Y. Iso, T. Isobe and H. Sasaki, *RSC Adv.*, 2017, **7**, 7936–7943.

21 K. Kim., S. Jeong, J. Y. Woo and C.-S. Han, *Nanotechnol.*, 2012, **23**, 065602.

22 T. Watanabe, C. Wada, Y. Iso, T. Isobe and H. Sasaki, *ECS J. Solid State Sci. Technol.*, 2017, **6**, R75–R80.

23 T. Watanabe, Y. Iso, T. Isobe and H. Sasaki, *RSC Adv.*, 2018, **8**, 25526–25533.

24 B. Wang, C. Zhang, S. Huang, Z. Li, L. Kong, L. Jin, J. Wang, K. Wu and L. Li, *ACS Appl. Mater. Interfaces*, 2018, **10**, 23303–23310.

25 H. Li, Y. Qian, X. Xing, J. Zhu, X. Huang, Q. Jing, W. Zhang, C. Zhang and Z. Lu, *J. Phys. Chem. C*, 2018, **122**, 12994–13000.

26 H.-C. Wang, S.-Y. Lin, A.-C. Tang, B. P. Singh, H.-C. Tong, C.-Y. Chen, Y.-C. Lee, T.-L. Tsai and R.-S. Liu, *Angew. Chem., Int. Ed.*, 2016, **55**, 7924–7929.

This journal is © The Royal Society of Chemistry 2019

*J. Mater. Chem. C*, 2019, **7**, 8546–8550 | **8549**

27  Z. Li, L. Kong, S. Huang and L. Li, *Angew. Chem.*, 2017, **129**, 8246–8250.

28  Y. Li, Y. Lv, Z. Guo, L. Dong, J. Zheng, C. Chai, N. Chen, Y. Lu and C. Chen, *ACS Appl. Mater. Interfaces*, 2018, **10**, 15888–15894.

29  T. Kosugi, Y. Iso and T. Isobe, *Chem. Lett.*, 2019, **48**, 349–352.

30  S. Huang, Z. Li, B. Wang, N. Zhu, C. Zhang, L. Kong, Q. Zhang, A. Shan and L. Li, *ACS Appl. Mater. Interfaces*, 2017, **9**, 7249–7258.

31  Y. Wang, X. Li, S. Sreejith, F. Cao, Z. Wang, M. C. Stuparu, H. Zeng and H. Sun, *Adv. Mater.*, 2016, **28**, 10637–10643.

32  S. Huang, Z. Li, B. Wang, N. Zhu, C. Zhang, L. Kong, Q. Zhang, A. Shan and L. Li, *ACS Appl. Mater. Interfaces*, 2017, **9**, 7249–7258.